Nearshore wave height variation in unsaturated surf

H.E. Power[1], M.G. Hughes[2], T. Aagaard[3] and T.E. Baldock[1]

[1] School of Civil Engineering, University of Queensland, St Lucia, QLD 4072, Australia

[2] School of Geosciences, University of Sydney, Sydney, NSW 2006, Australia

[3] Institute of Geography and Geology, University of Copenhagen, Oster Voldgade 10, DK-1350 Copenhagen K., Denmark

Abstract

The nearshore evolution of wave height is presented from field observations during unsaturated surf conditions from 10 different beaches characterized by micro-tidal conditions and predominantly swell dominated wave climates. Wave evolution is presented in terms of wave height to water depth ratio (γ) for comparison with previous data from saturated surf. Both conventional time-averaged (γ_{rms}) and a new wave-by-wave analysis (γ_w) are performed. Values of γ increase with increasing offshore wave height, indicating unsaturated surf. The observations show a variation in γ-values from near constant values in the mid-surf zone to rapidly and asymptotically increasing γ-values in the inner surf zone. In contrast to previous data from saturated surf, γ shows no dependence on either the absolute beach slope or the relative beach slope, $\beta / k\bar{h}$. The skewness of the distributions of γ_w is consistent with waves that are not depth-limited. The inner surf zone wave heights are approximately equally dependent on the water depth and offshore wave height. The previous observations of γ from saturated surf are shown to be consistent with a terminal bore height at the shoreline which is in excellent agreement with a previously derived value for the Miche parameter. In contrast, for the present unsaturated surf conditions, the terminal bore height at the shoreline can be approximated by $H_b \approx 0.12 H_o$, which is consistent with recent laboratory data sets.

1. Introduction

The hydrodynamics of the inner surf zone are an important component of the forcing within the nearshore zone. In particular, the inner surf conditions are important boundary conditions for the beach and swash zone [*Battjes*, 1988; *Brocchini and Baldock*, 2008] and therefore the exchange of sediment between the sub-aerial and sub-tidal coastal zones [*Masselink and Puleo*, 2006]. Waves in the the inner surf zone generate significant near bed velocities and turbulence, and are very effective at suspending and advecting sediment. Suspended sediment concentrations and sediment transport rates in this region are usually large [*Aagaard and Masselink*, 1999; *Kobayashi and Johnson*, 2001; *Kobayashi et al.*, 2008]. The dynamics of the inner surf zone also have a direct impact on nearshore water levels and wave setup at the beach face [*Nielsen*, 1989; *Raubenheimer et al.*, 2001; *Dean and Dalrymple*, 2002; *Apotsos et al.*, 2007] where the impacts of beach erosion are most pronounced [*Hughes and Turner*, 1999]. In addition, in many beach morphology models wave height variation is a key parameter [e.g. *Dean*, 1991; *Srinivas and Dean*, 1996].

Extensive laboratory experiments with monochromatic waves suggest that waves are usually depth-limited, such that the wave height is directly proportional to the water depth [see *Nielsen*, 2009, for a recent overview]. Field experiments have indicated that waves in the inner surf zone may be saturated, such that wave height (H) is a function of water depth (h) and relative beach slope, and independent of offshore wave height (H_o) [*Raubenheimer et al.*, 1996; *Sénéchal et al.*, 2001; *Sénéchal et al.*, 2005]:

$$H = C_o h + C_1 \frac{\beta}{k} \tag{1}$$

where C_0 and C_1 are constants, β is the local beach gradient and k is the local wavenumber. The relationship is more often written in terms of the ratio of the significant sea-swell wave height to local water depth, γ_s:

$$\gamma_s = C_o + C_1 \frac{\beta}{kh}. \tag{2}$$

Wave height to water depth ratios, γ, in the surf zone and as a breaker criterion, γ_b, are important in many wave transformation models [*Battjes and Janssen*, 1978; *Thornton and Guza*, 1983; *Ruessink et al.*, 2003; *Alsina and Baldock*, 2007; *Janssen and Battjes*, 2007] and therefore in the prediction of run-up, radiation stresses and nearshore circulation. Different studies have found varying values for γ and γ_b - from as low as 0.32 up to 1.2 [*Sallenger and Holman*, 1985] - and the values have also been shown to be correlated with a number of factors including beach slope and wave steepness [*Battjes*, 1974; *Weishar and Byrne*, 1978; *Battjes and Stive*, 1985; *Sallenger and Holman*, 1985; *van der Westhuysen*, 2010].

Raubenheimer *et al*. [1996] proposed the form of γ_s given by (1) and (2), where wave heights are still saturated (independent of H_o) even though γ_s increases rapidly in shallow water. Although Raubenheimer *et al*. [1996] use the terms depth-limited and saturated interchangeably, (1) is consistent with saturation, but wave heights are not solely a function of the water depth. Here, depth-limited waves are defined as those whose height is solely dependent on the water depth. Saturated surf zone is defined as conditions where time-averaged wave heights are independent of the offshore wave height. Unsaturated surf is defined as conditions where an increase in offshore wave height leads to an increase in surf zone wave height. Depth-limited waves, by definition, imply saturation, but waves are not necessarily depth-limited in a saturated surf zone. Nevertheless, Eqs (1) and (2) are appealing since they imply a finite wave height at the shore, consistent with short wave swash forced by bores [e.g. *Hughes*, 1992; *Baldock and*

Holmes, 1999; *Puleo et al.*, 2003]. In Section 5, this is considered further and we show that this functional form for γ is consistent with the value of the Miche parameter for saturated swash and inner surf conditions derived by Baldock and Holmes [1999].

As a result of these field studies, waves in the inner region of the surf zone are usually assumed to be saturated or depth-limited [see *Komar*, 1998, for review]. However, this assumption is based on data from a limited range of conditions and beaches [e.g. *Thornton and Guza*, 1982; *Wright et al.*, 1982; *Sallenger and Holman*, 1985; *Raubenheimer et al.*, 1996; *Sénéchal et al.*, 2005]. Even though the concept of depth-limited and/or saturated wave heights in the inner surf zone appears applicable to highly dissipative beaches (because there is more time for waves to adjust to changes in depth), it has not been confirmed on all beach types. Further, the concept is usually applied to time-averaged wave heights (usually derived from the sea-swell variance), which implies the time-averaged wave height and wave celerity at the shoreline tend to zero. This explicitly implies that there is no short-wave driven swash, which is inconsistent with observed swash sediment transport modes [*Horn and Mason*, 1994]. Similarly, for waves that are depth-limited, neither amplitude dispersion nor wave overtaking can occur (since frequency dispersion is assumed negligible in shallow water), but wave overtaking is common on natural beaches [*Peregrine*, 1974; *Bradshaw*, 1982]. Measurements and modeling by Goda [1975] demonstrated that surf zones are not necessarily saturated on steep or mild slopes, with shoreline wave heights dependent on offshore conditions. On steep foreshores, laboratory experiments also show that the inner surf zone can be unsaturated, with wave heights dependent on offshore wave heights [*Baldock et al.*, 1998].

Nearshore wave height variation, and the applicability of a depth-limited wave model, on steeper intermediate beach types has not been considered in most previous field experiments, particularly in the inner surf zone. This paper addresses this issue and presents a very comprehensive data set from ten different sandy beaches that encompass a wide range of beach types, beach slopes and wave conditions that the data show was typically unsaturated surf. The data set is compared to the most common method used to calculate γ-values (γ_{rms}) and shows significant differences from the data presented by Raubenheimer *et al*. [1996] and Sénéchal *et al*. [2005] for saturated surf conditions. The data show additionally that time-averaging masks significant detail in the data, such that while the mean γ-values remain strongly dependent on water depth, individual wave heights are not constrained to the same extent. To enable a more detailed investigation of γ-values for individual waves, a new method of wave-by-wave analysis is outlined and, using this method, two alternate forms of γ for individual waves are proposed for different definitions of the water depth. The latter of these suggests a limiting value of γ at the shore, consistent with the present observations.

The field sites, data collection and data pre-processing are described in Section 2. Section 3 contrasts the present data from unsaturated surf with that presented by Raubenheimer *et al*. [1996] for saturated surf, using the same analysis methods, and presents the results from a wave-by-wave analysis of γ-values. Section 4 provides a discussion of the data and includes the derivation of theoretical values for C_1 in (1) and (2), and which are consistent with the values proposed by Raubenheimer *et al*. [1996] and Sénéchal *et al*. [2005]. Final conclusions follow in Section 5.

2. Methods

2.1. Field sites

This study presents experimental data obtained from the inner surf zones of 10 different sandy beaches during 27 different instrument deployment periods over individual tidal cycles (e.g. 12 hours or less; Table 1, Fig. 1). The instrument deployments include data from a large range of beach types (from reflective to dissipative; see [*Wright and Short*, 1984]), and from both sea and swell conditions. The majority of the deployments (24 of 27 instrument deployments) were collected from the southeast coast of Australia, which is characterized by micro-tidal beaches with moderate, swell dominated wave climates. The remaining three deployments were collected at Vejers Beach, Denmark, which is a micro-tidal sandy beach, characterized by a moderate sea wave climate [*Aagaard et al.*, 2008]. The majority of the data collected is from the inner surf zone (see 2.3). Instruments were located within 20-40m of the shoreline and the surf zone widths were in the range 50-400m indicating that the majority of sensors were located within the inner surf zone (see Section 2.3). Furthermore, visual observations of waves at all sensors confirmed that the vast majority of waves were broken, although unbroken waves can remain present until the shoreline, consistent with a Rayleigh pdf for nearshore wave heights [*Thornton and Guza*, 1983; *Baldock et al.*, 1998]. Offshore wave data was obtained from wave buoys in depths ranging from 16-85m. Directional wave data was not available at all sites o a correction back to deep water cannot be applied consistently. Hence, significant offshore wave height, H_o, is taken as the offshore condition at the wave buoys.

2.2. Experimental setup

In each deployment, pressure transducer (PT) data were collected from multiple cross-shore locations within the inner surf zone, with the number of PTs located in the inner surf zone at one time ranging from 1 to 14. In the majority of deployments, PTs were located on the bed. In all other cases, the elevation of the PTs relative to the bed was surveyed and PT data are converted to water surface elevations above the bed. Data were recorded at sampling rates that ranged from 4 to 10Hz. The beach profile and instrument locations were surveyed at least once during each deployment and in many cases surveys were conducted at both the beginning and end of each deployment. The deployment conditions, including sampling frequency, the maximum number of PTs in the inner surf zone in one data record, and the total number of data records for each deployment are listed in Table 1.

2.3. Data pre-processing

Prior to full data analysis, all raw pressure transducer records were divided into 15-minute time series to ensure stationarity with respect to the changing tidal water level [*Hughes and Moseley*, 2007]. Subsequently, each 15-minute data record was visually checked to identify if the PT was located in the surf or swash zone. Data records that contained sections of the time series where the PT became dry were taken to be within in the swash zone and were removed from the data set. Hence, the later analysis presents data collected from PTs that were submerged for the full duration of each 15 minute data record. All time series were low pass filtered at 1Hz to remove instrument noise prior to further analysis.

To further confirm that the data was collected from the inner surf zone, mean water depth ($\overline{h}$) normalized by H_o was calculated for each data record (Figure 2). For a dissipative surf zone, the breaker index at the breakpoint ($\gamma_{br} = H_{sig}/\overline{h}$ where H_{sig} is significant wave height) is approximately 0.5 [*Thornton and Guza*, 1982; 1983; *Raubenheimer*, 2002, their Figure 4]. This is in agreement with the data of Ruessink *et al*. [1998] that indicated that the largest waves in a wave group start to break at $\bar{h}/H_{sig} = 3$, thus defining the seaward limit of the outer surf zone. If there is negligible shoaling and refraction such that $H_{sig} \approx H_o$, then the outer surf zone can be defined as occurring in the range $\bar{h}/H_{sig} = 2-3$, consistent with the observations of Thornton and Guza [1983] and Ruessink *et al*. [1998]. Based on this, all the data used was from landward of the outer breakpoint. Additionally, over 60% of the data have $\bar{h}/H_o < 1$, indicating they were obtained from the shallower water depths of the surf zone, i.e. the inner surf zone, and over 80% has $\bar{h}/H_o < 1.5$, indicating they were collected from landward of the mid-surf zone (Figure 2).

2.4. Calculation of time-averaged γ-values

The most common method to calculate wave height to water depth ratios, γ-values, is to use the root-mean-square wave height, H_{rms}, calculated using the variance (m_o) of the high-pass filtered water surface elevation, and $\bar{h}$ such that

$$H_{rms} = \sqrt{8m_o} \tag{3}$$

and

$$\gamma_{rms} = \frac{H_{rms}}{\bar{h}} \tag{4}$$

[*Thornton and Guza*, 1982; *Wright et al.*, 1982; *Thornton and Guza*, 1983; *Sallenger and Holman*, 1985; *Sallenger and Howd*, 1989; *Masselink and Hegge*, 1995]. The estimate of H_{rms} from (3) has been shown to be within 20% of the H_{rms} value determined from wave-by-wave analysis owing to the non-linearities which are not taken into account by assuming linear waves [*Thornton and Guza*, 1982].

Raubenheimer *et al.* [1996] adopted an alternative but consistent measure, using H_s instead of H_{rms}, and defining

$$\gamma_s = H_s / \bar{h} \tag{5}$$

where $H_s = \sqrt{16m_o}$. Raubenheimer *et al.* [1996] observed a trend between γ_s and the normalized beach slope, defined as $\beta / k\bar{h}$ (denoted here as $\beta / k_{pf}\bar{h}$). Such a correlation is tested for the present data, using the same analysis method. For this, the data were band-pass filtered from 0.05-0.18Hz in accordance with the pre-processing of Raubenheimer *et al*. [1996]. The parameter k (denoted here as k_{pf}) was calculated using the shallow water approximation to the hyperbolic tangent equation for wavelength, where $k_{pf} = 2\pi / L$, the wavelength L was calculated using $L = CT_{pf}$ where T_{pf} is the peak spectral wave period calculated using the filtered energy spectra and wave celerity C is given by $C = \sqrt{g\bar{h}}$, where g is the gravitational constant. For the wave periods in this study, this approximation is valid in water depths ca. $\bar{h} < 2$m, which is satisfied for over 98% of the individual waves within the data set. The value used for β is local beach slope between two adjacent PTs, on the seaward side if available.

2.5. Wave-by-wave analysis

In order to investigate the characteristics of individual waves, as opposed to time-averaged wave conditions, wave heights, water depths, and wave height to water depth ratios are also calculated for each individual wave within the data records. Traditionally, in relatively deep water, individual wave heights and wave periods are determined from a zero crossing analysis.

However, in shallow water, the results from these methods are very sensitive to the definition of the mean water level about which the zero crossings are defined (Figure 3). Due to the presence of long waves and other low frequency motions in the inner surf zone, the results from a zero crossing analysis are strongly dependent on whether or not the original data record is filtered to extract only sea-swell frequencies. If a zero crossing analysis is conducted on an unfiltered data record that has strong long wave oscillations, the long waves can cause incident short wave troughs to occur above the mean water level and short wave crests to occur below the mean water level which causes these waves to be missed in the analysis. This would be the case for the two waves shown in Figure 3a that occur between 380 and 400s as the trough between the two waves occurs above the mean water level.

Given that sea and swell waves are the focus of the analysis, the usual approach would be to filter the data records to remove the low frequency motion (infragravity waves). Unfortunately, since the filtering is a linear process applied to a non-linear system, the filtering process appears to dramatically alter the shape of the waves in some circumstances. For example, comparing the unfiltered (Figure 3a) and high-pass Fourier filtered (Figure 3b) data records shows that at t=380-390s and t=420-440s the short wave shape, period and wave height have altered significantly. Further, the mean water level experienced by individual waves is dependent on the low frequency or infragravity waves, as is also illustrated in Figure 3a. Such water level variations should be retained in the analysis when determining γ-values.

Given the inherent problems with the filtered zero crossing analysis outlined above, an alternative approach for wave-by-wave analysis in the surf zone has been developed. This method identifies the wave troughs (local minima) in the data record and defines an individual wave between two consecutive troughs. Using this local minima analysis, a wave-by-wave analysis can be undertaken without filtering the data record and, therefore, without altering the wave shapes and water depth variations experienced by individual waves. To avoid classifying ripples and small wavelets as individual waves, oscillations with a period less than one-quarter of the peak spectral wave period calculated using the entire spectrum (T_p) at each sensor are removed from the analysis. Figure 3b shows an example data record and the waves selected by the local minima analysis. For the present data, a zero-crossing and the local minima analysis give very similar results for mean (record averaged) γ-values. However, there are significant differences in H_{rms}, and hence γ, for individual waves, as well as differences in T which is important in determining relative beach slope (see Figures 6f and 7c).

3. Results

3.1. Variation of time-averaged γ_{rms} and γ_s

For each deployment, time-averaged γ_{rms}-values were calculated as specified by (4). Figure 4a illustrates the trend of γ_{rms} with H_o, showing an increase in γ_{rms} with increasing H_o. This trend is consistent for the lower and upper bounds of the data, as well as the mean. Since there is a strong correlation between γ and water depth (see Section 3.3), Figure 4b shows the same data separated into bins from different mean water depths. The same trends are evident, particularly for offshore wave heights in the range 0.5-2m, and these conditions encompass the majority of the data set and the typical wave conditions for these coasts. In addition, for a given offshore wave height, a wide range of γ_{rms}-values were observed. Both observations suggest that wave heights are not depth-limited. For the present data, Figure 4 clearly shows that γ-values increase with increasing H_o, indicating that wave heights are unsaturated and consequently not depth-limited. Note that since γ also varies strongly with water depth, a range of γ for a given H_o is not sufficient to define waves as unsaturated. In contrast, from (1), a range of γ is sufficient to define wave heights as not depth-limited.

Raubenheimer *et al.* [1996] showed a strong correlation between γ and cross-shore location, with γ increasing further shoreward, and attributed the dependence to variations in beach gradient (β generally increasing shoreward except in a bar-trough) and specifically $\beta \big/ k_{pf}\overline{h}$, as indicated in (1). A similar trend between γ and cross-shore location is also clear in the present data. For the present unsaturated wave data, however, γ is strongly dependent on the water depth rather than the relative change in depth. Figure 5 illustrates the dependence of γ on water depth for six different field deployments from five different beaches. In all cases there is a gradual shoreward increase in γ in the deeper water depths, and the rate of change increases as the water shallows. In the deeper water depths, where γ_{rms} varies slowly, γ_{rms}-values were around 0.2 to 0.4, which is consistent with previous research (see Section 1). In the inner surf zone, for depths less than about 1m, γ_{rms} increased rapidly, and root-mean-square wave heights were almost equal with the mean water depth in some deployments.

Since beach slope does generally increase shoreward for most beaches, this trend could be consistent with that observed by Raubenheimer *et al*. [1996]. Performing the same data analysis as Raubenheimer *et al*. [1996] on the present data set (i.e. band-pass filtering from 0.05-0.18Hz) yields a similar trend to that proposed by Sénéchal *et al*. [2005], but one which is also much flatter (Figure 6a). Since β may be a function of water depth, and k_{pf} is a strong function of depth, the correlation between γ_s and the individual parameters in (1) and (2) was investigated further, and is also shown in Figure 6. For the present data, γ_s is clearly not well correlated with local beach slope (Figure 6b). Further, a comparison between β and $\overline{h}$ for each data record from all 27 deployments demonstrates no correlation between β and $\overline{h}$, with a large range of beach slopes observed at each mean depth (not shown). From Figures 6c-f, it is clear that γ_s is inversely correlated with depth (but scattered over a significant range) and approximately linearly correlated with k. However, for shallow water waves, k_{pf} is strongly dependent on the water depth and therefore not an independent parameter. Plotting γ_s versus the (independent) peak spectral period (T_{pf}) shows no correlation. This therefore suggests that the wavelength is not an important parameter in determining the nearshore variation of γ_s for these data and that the correlation of γ_s with k_{pf} is due to its dependence on $\overline{h}$. Consequently, the correlation of the relative change of depth with γ_s seems to reflect the relationship between γ_s and $\overline{h}$ rather than the other parameters.

Therefore, despite showing a similar trend between γ_s and $\beta / k_{pf}\overline{h}$ to the data of Raubenheimer *et al*. [1996], the present data show no physical dependence on relative beach slope.

This is further confirmed when the above analysis is repeated using the data obtained using the local minima analysis to obtain values of the mean wave period ($\overline{T}$; Figure 7). Using $\overline{T}$ instead of T_{pf} results in a much wider range of values for the wave period (Figure 7c) and hence a wider range of values for wavenumber (Figure 7b). As a result of this, no trend is observed between γ_s and $\beta / \overline{k}\overline{h}$ (Figure 7a), indicating that the previous trend for these data is due to the effect of filtering.

3.2. Wave-by-wave analysis of γ

Previous analyses of γ-values from field data have focused on time-averaged values as described above. This is appropriate if the variation of individual wave heights at one location (constant h) is small. If waves are not depth-limited and not saturated, however, then considerable variation of individual wave heights and γ-values is to be expected at constant h. This is investigated using the wave-by-wave analysis procedure described in Section 2.5. For individual waves, two different definitions of the water depth are possible, which reflect the different physical characteristics of non-breaking waves and fully developed surf zone bores. Firstly, a γ-value can be calculated for each individual wave using the trough depth, h_{tr}, preceding that wave:

$$\gamma_{tr} = \frac{H}{h_{tr}} \tag{6}$$

This definition of γ_{tr} using h_{tr} is advantageous for two reasons; firstly it excludes the wave height from the water depth (which becomes significant in very shallow water close to the surf-swash boundary), and secondly, it uses the preceding water depth that governs the propagation and dissipation of fully developed bores [e.g. *Peregrine*, 1983]. Secondly, a γ-value can be calculated using the mean depth over the wave period, h_w,

$$\gamma_w = \frac{H}{h_w} \tag{7}$$

where h_w is calculated as the mean water depth between two consecutive troughs, which is consistent with the definition of an individual wave using the local minima analysis. The advantage of this definition is that γ_w can still be defined robustly for waves that have small or zero values of h_{tr}, i.e. waves at the shoreline. Assuming that the variation in bore surface elevation at the shoreline can be approximated by a simple triangular shape [*Brocchini and Baldock*, 2008], this provides a sensible limiting value for γ_w at the shoreline, i.e. h_w=H/2, giving γ_w = 2 at h_{tr}=0. The individual γ-values obtained from (6) and (7) can be record-averaged over a 15-minute data record (i.e. $\overline{\gamma}_{tr}$ or $\overline{\gamma}_w$) or analyzed further as individual γ-values, for example to construct a probability density distribution. Note that few waves have γ_w-values that approach 2 since the present data sets only include data records where the minimum trough depth is always greater than zero. The γ-values for individual waves within the surf-swash transition zone, i.e. above the run-down limit for that data record, will be considered in a later paper.

3.3. Variation of time-averaged γ with relative water depth

A comparison between the γ-values obtained from (4), (6) and (7) is illustrated in Figure 8. The water depths have been normalized by the offshore wave height, H_o, to account for the unsaturated nature of the surf conditions and to allow data comparison at the same relative depth or surf zone position. The γ-values calculated on a wave-by-wave basis and then record-averaged ($\overline{\gamma}_w$ and $\overline{\gamma}_{tr}$, Figure 8c-f) show significantly greater increases in the inner surf zone than γ_{rms}, with these γ-values approximately twice the γ_{rms}-values observed in the same depth despite γ-values being approximately equal in deeper water.

Figure 9 shows record-averaged γ_{tr}- and γ_w-values ($\overline{\gamma}_{tr}$ and $\overline{\gamma}_w$) for all data (i.e., all data records and all beaches) plotted against $\overline{h}_{tr}$ and $\overline{h}_w$ normalized by the offshore significant wave height (H_o). The data show a very consistent pattern and strong dependency on the relative water depth. In all deployments, both $\overline{\gamma}_{tr}$- and $\overline{\gamma}_w$ increased shoreward in the surf zone, showing similar trends to γ_{rms} (Figure 5). Both $\overline{\gamma}_{tr}$- and $\overline{\gamma}_w$- values increased slowly in the shoreward direction in the mid-surf zone and then rapidly increased in the shallower water depths close to the shoreline. In the shallower water depths, $\overline{\gamma}_{tr}$ occasionally reached values greater than two, although a maximum value of one was more usual before the sensors entered the swash zone at some point of the recording period. For deployments where there was a change from slowly increasing to rapidly increasing $\overline{\gamma}_{tr}$, this change occurred at a relative depth $\overline{h}_{tr}/H_o$ of approximately 0.5 (Figure 9a). In all remaining deployments no region of slowly increasing $\overline{\gamma}_{tr}$ was observed, only rapidly increasing $\overline{\gamma}_{tr}$. However, in all these deployments, no data records had $\overline{h}_{tr}/H_o$ greater than 0.5.

As discussed in Section 3.2, as $\overline{h}_{tr}$-values approach $\overline{h}_{tr}$=0, $\overline{\gamma}_{tr}$-values increase asymptotically, i.e. a finite bore height remains at the shoreline. Similarly, as $\overline{h}_w$-values approach $\overline{h}_w$ =0, $\overline{\gamma}_w$-values approach $\overline{\gamma}_w$=2. The relationship between $\overline{\gamma}_{tr}$ ($\overline{\gamma}_w$) and $\overline{h}_{tr}$ ($\overline{h}_w$) from all deployments clearly demonstrates that γ-values are related to absolute, and also relative, water depth. An alternative representation for these data is illustrated in Figure 10, where $\overline{\gamma}_w$ is plotted versus $\overline{h}_{tr}/\mathrm{H_o}$ for each data record. In this instance, if a sawtooth bore shape is assumed at the shoreline, then the expected shallow water limit is $\bar{\gamma}_w$=2 at $\bar{h}_{tr}$/H_o=0, which is in good agreement with the data. An empirical curve with these parameters:

$$\gamma_w = \frac{2}{(1+20\bar{h}_{tr}/H_o)^{0.75}} \tag{8}$$

provides a good fit to the data (R^2=0.77).

3.4. *γ*-values for individual waves

Taking the resulting individual γ_{tr}- and γ_w-values for each wave, the distributions of wave-by-wave γ_{tr} and γ_w for each data record was calculated, and two examples are shown in Figure 11. For each data record (approximately 100 waves) the skewness of the distribution of individual γ-values (γ_{tr} and γ_w) was calculated and the results for all records are illustrated in a histogram in Figure 12. Distributions of γ_{tr} were generally not skewed, with more than 30% of all data records with skewness values in the range -0.1 to 0.1 and more than 95% of all data records with skewness values in the range -0.5 to 0.5. The distributions of γ_w-values showed similar results (not shown). This indicates that, for the majority of data records, the distributions of γ_{tr}- and γ_w-values are approximately symmetric, suggesting that there is no strong upper limit to wave height to water depth ratios, i.e. individual wave heights are not severely limited by the water depth. While the γ distributions for individual waves within one data record were generally not skewed, the overall distributions of both γ_{tr}- and γ_w-values for all data (every individual wave in the data set) are positively skewed, very strongly so for γ_{tr}; the γ_{tr}-values have a skewness of > 300 and the γ_w-values have a skewness of 1.5 (Figure 13). This indicates that in the data set on average, there are very few waves with large γ-values and a large number of waves with small γ-values. Since depth-limited waves should be negatively skewed due to the truncated distribution, this demonstrates that the present data are inconsistent with such a model. Modeling the cross-shore variation and skewness of γ is necessary to predict wave height distributions [*Battjes and Groenendijk*, 2000].

To further illustrate the variation of γ-values in one data record, individual wave heights recorded at each cross-shore sensor are plotted against water depth (both h_w and h_{tr}) for selected and representative data records (Figure 14). Data from the same sensor (cross-shore location) are shown in the same color. The observations show that there is no well-defined upper limit that wave heights consistently reach, but do not exceed, and that the wave heights trend toward a finite value at the shore. This is the case even for deployments where the time averaged values of $\overline{\gamma}_{tr}$ shows a very distinct relationship with $\overline{h}/H_o$ (e.g. Figure 8d and Figures 12e-f).

4. Discussion

The results of this study are based on the analysis of over 2000 15-minute time series of waves within the inner surf zone from 10 different sea- and swell-dominated beaches that span a range of beach types and where inner surf zone beach face gradients range from 0.014 to 0.087. Time-averaged wave height to water depth ratios (γ-values) have been calculated using the method that has been used in the majority of previous studies [γrms, e.g. *Battjes*, 1974; *Weishar and Byrne*, 1978; *Sallenger and Holman*, 1985; *Raubenheimer et al.*, 1996]. Consistent with observations from saturated surf [*Raubenheimer et al.*, 1996], the present results show that γ_{rms} is relatively constant in the outer parts of the inner surf zone, but increases rapidly further landward and that γ_{rms} was not a constant, which is in contrast with a number of previous studies [e.g. *Thornton and Guza*, 1982; 1983]. This observation suggests that in the mid-surf zone, energy dissipation from wave breaking can keep up with the decreasing water depth, but in the inner surf zone wave energy dissipation cannot keep up with the rapidly decreasing water depth, leading to a rise in γ-values. A possible reason is that dissipation is proportional to H^3/h and as a result, smaller waves dissipate proportionally less energy. This behavior can be predicted by some parametric wave transformation models [e.g. *Svendsen*, 1984; *Baldock et al.*, 1998; *Ruessink et al.*, 2003; *Alsina and Baldock*, 2007; *Janssen and Battjes*, 2007], and therefore the assumption of constant wave height to water depth ratio in many wave transformation models is not necessary. A gradational breaker index [*Goda*, 2004] has also been used to derive a parametric wave transformation model for these conditions.

The nearshore behavior of γ-values has also been investigated on a wave-by-wave basis for the first time. Two new definitions for γ have been proposed for individual waves in the inner surf zone, γ_{w} and γ_{tr}, which depend on the definition of water depth for individual waves. While the overall trend of γ_w, γ_{tr} and γ_{rms} are similar, record-averaged values of the wave-by-wave parameters, $\overline{\gamma}_{tr}$ and $\overline{\gamma}_w$, show much greater increases in the inner surf zone than the γ_{rms}-values. Averaged γ-values for individual waves are up to twice the γ_{rms}-values. This suggests that for unsaturated surf zones γ_{rms} does not accurately reflect the extent to which individual wave heights increase relative to water depth in the inner surf zone. Values of $\overline{\gamma}_{tr}$ increase asymptotically toward the shore, indicating non-zero wave height at the shoreline. The parameter $\overline{\gamma}_w$ has a theoretical limit of $\overline{\gamma}_w = 2$ at the shoreline, which is consistent with the observations and also with non-zero wave height at the shoreline. These observations of non-zero wave height at the shoreline provide a model for wave-runup and swash driven by sea and swell waves, which is consistent with observations on the majority of beach types, but inconsistent with the depth-limited conceptual short wave model. Individual wave heights and γ-values show significant variation within individual data records, with no defined upper threshold, again suggesting that individual waves were not depth-limited. Consequently, to accurately describe energy dissipation from breaking waves, a continuous wave height distribution [*Baldock et al.*, 1998; *Alsina and Baldock*, 2007; *Janssen and Battjes*, 2007] appears more appropriate for parametric modeling of unsaturated surf zones than the classical truncated distribution [*Battjes and Janssen*, 1978].

Previous studies have demonstrated that γ is dependent on beach slope or relative beach slope [e.g. *Sallenger and Holman*, 1985; *Raubenheimer et al.*, 1996; *Sénéchal et al.*, 2005] in saturated surf. This trend was also observed in the present unsaturated surf zone data. However, here it can clearly be attributed to the dependence of γ on $\overline{h}$ rather than any correlation with wave period. A correlation exists between γ and k_{pf}, but this is due to the correlation between $\overline{h}$ and k_{pf}. Raubenheimer *et al.* [1996] observed high γ_s-values (1.2-1.4) for high values of $\beta / k_{pf}\overline{h}$

(0.9-1.0), which is very different from those observed in this study (γ_s=0.4-0.8) for the same range of $\beta/k_{pf}\overline{h}$ (Fig. 6). High values of $\beta/k_{pf}\overline{h}$ indicate steeply sloping beaches, shallow water depths and large wavelengths (long wave periods). It is possible that the high γ-values observed by Raubenheimer *et al.* [1996] are due to the presence of shore-breaks at one of their field sites, as reported in their study. It is currently unknown why relative beach slope plays a more important role in saturated surf zones than unsaturated surf zones, however, the importance of offshore wave height in unsaturated surf zones may conceal any effect due to relative beach slope.

It should be noted that the parameter γ and γ_b represent very different ratios of wave height to water depth and that they are also obtained differently, and therefore they can exhibit opposite trends. For example, these data, and that of Raubenheimer *et al*. [1996] and Sénéchal *et al*. [2005], show that γ increases in shoreward. Conversely, Ruessink *et al*. [2003], found that γ_b decreased shoreward. However, Ruessink *et al*. were optimising γ_b to provide the best fit between field data and the parametric wave transformation model of Baldock *et al*., [1998], which includes γ_b as a free parameter, and a decreasing γ_b was required to achieve sufficient energy dissipation in nearshore sandbar troughs. Very recently, van der Westhuysen [2010] applied the original wave transformation model of Battjes and Janssen [1978] and derived a new parameterisation for γ_b that also reduces in shallow water. It is worth noting that Janssen and Battjes [2007] and Alsina and Baldock [2007] recently modified the Baldock *et al*. [1998] model to increase the rate of energy dissipation in shallow water. Consequently, optimizing γ_b with this new model may not require a reduction in γ_b in order to match observations of wave height decay close to the shoreline.

Since the present data were obtained from unsaturated surf, γ should be correlated with offshore wave height in addition to water depth. This is illustrated in Figure 15. The least-squares linear fit gives

$$\gamma_w = 0.11 H_o / h_w + 0.11 \tag{9}$$

with $R^2 = 0.73$ and the best fit power curve gives:

$$\gamma_w = 0.22 \left(H_o / h_w \right)^{0.63} \tag{10}$$

with R^2=0.74. From (9) it is apparent that the wave height is approximately equally dependent on the local water depth and offshore wave height as this can be rewritten as $H = 0.11 H_o + 0.11 h_w$. Note that (9) is only valid for finite H_o, since γ should be zero if H_o is zero, but gives a better fit to the data as the depth tends to zero.

Finally, it is of interest to consider why the data of Raubenheimer *et al*. [1996] show a dependence on relative beach slope. Since their data was from saturated surf, the swash would also be saturated [*Ruggiero et al.*, 2004]. Baldock and Holmes [1999] derived values of the Miche parameter, ε, for the saturated swash amplitude, a_s, and for the terminal bore amplitude, a_b, that leads to swash saturation by breaking waves:

$$\varepsilon = \frac{a \omega^2}{g \beta^2} \tag{11}$$

where $\omega = 2\pi / T$, and $\varepsilon_s \approx 2.5$ for the swash amplitude or $\varepsilon_b \approx 1.25$ for the terminal bore amplitude. At the shoreline (swash boundary) in saturated surf, the wave amplitude in (11) should be consistent with that in (1) and the constant C_1 can be derived. Taking (1) and substituting for $k = 2\pi / T\sqrt{gh}$ gives:

$$H_b = C_o h + C_1 \frac{\beta T \sqrt{gh}}{2\pi} \tag{12}$$

For the data of Raubenheimer *et al*. [1996] and the definition of γ, $\gamma \approx 1$ at the shoreline, so $h=H_b$, giving:

$$H_b(1-C_o)^2 = \frac{C_1^2 g\beta^2}{\omega^2}. \tag{13}$$

From (11),

$$\frac{H_b\omega^2}{g\beta^2} = 2\varepsilon_b \approx 2.5 \tag{14}$$

Rearranging (13) and substituting from (14) gives:

$$C_1^2 = \frac{(1-C_o)^2 H_b\omega^2}{g\beta^2} = 2\varepsilon_b(1-C_o)^2 \tag{15}$$

From Raubenheimer *et al*. [1996], C_o=0.19±0.09, which from the results of (11) gives a theoretical mean value for $C_1 \approx 1.28$, and a range of $1.14<C_1<1.42$. Raubenheimer *et al*. [1996] found C_1=1.05±0.15 from their best fit to (1) and (2), in agreement with (15). A similar result can be derived for the data of Sénéchal *et al*. [2005] which showed γ-values approximately twice those of Raubenheimer *et al*. [1996]. Completing the above analysis with $\gamma \approx 2$ at the shoreline gives:

$$C_1^2 = 2\varepsilon_b(2-C_o)^2 \tag{16}$$

Using C_0=0.35 from Sénéchal *et al*. [2005] gives a theoretical value of $C_1 \approx 2.61$, which is again consistent with the value ($C_1 \approx 2.18$) derived from the observations. Thus, for a saturated surf zone, wave heights are saturated (independent of H_o), but not necessarily depth-limited, i.e. a finite terminal bore height occurs at the shoreline. Further, the theoretical finite terminal bore height for saturated inner surf and swash conditions [*Baldock and Holmes*, 1999] is in good agreement with the data of Raubenheimer *et al*. [1996] and that of Sénéchal *et al*. [2005]. In contrast, for the present data, the terminal bore heights are unsaturated and therefore not dependent on the inner surf and swash zone beach slope or the wave period. For these data, using (9) and substituting $h_w = H/2$ gives the terminal bore height as $H_b \approx 0.12 H_o$. This value is consistent with the random wave data presented by Baldock and Huntley [2002], their Figure 3, and Battjes *et al*. [2004], extrapolating the data in their Figure 2, as well as design charts presented by Goda [1975; 1998].

5. Conclusions

Comprehensive field measurements of the nearshore evolution of wave height are presented for unsaturated surf conditions. The data were obtained from 10 different beaches under a large range of sea and swell conditions, and include over 215,000 individual waves. Wave evolution is presented in terms of wave height to water depth ratio (γ) for comparison with previous data from saturated surf conditions. Both conventional time-averaged and a wave-by-wave analysis were performed. The observations show a variation in γ-values from near constant values in the mid-surf zone to rapidly increasing γ-values in the inner surf zone, with an asymptotic increase as the shoreline is approached. The wave-by-wave analysis suggests a limiting value for γ_w=2 at the shoreline, consistent with a simple model for the temporal variation of water depth for fully developed bores reaching the swash zone boundary. The transition between relatively constant and rapidly varying wave height-water depth ratios occurs at a relative water depth, h_w/H_o, of approximately 0.5. In contrast to previous data from saturated surf [*Raubenheimer et al.*, 1996; *Sénéchal et al.*, 2005], γ shows no dependence on either the absolute beach slope or the relative beach slope, $\beta/k_{pf}\overline{h}$. The γ-values for individual waves, γ_{tr} and γ_w, show similar trends to the time-averaged values, γ_{rms}, but the means of values for individual waves are consistently greater. The skewness of the distribution of γ for individual waves within a data record is generally small and the distribution of γ for all individual waves is positively skewed. Both observations are consistent with waves that are not depth-limited. Taking the observations as a whole, the observations show that the inner surf zone wave heights are approximately equally dependent on the local water depth and offshore wave height. Finally, for saturated surf, we show that the previous observations of Raubenheimer *et al*. [1996] are consistent with a theoretical terminal finite bore height at the shoreline, which is in excellent agreement with the value of the Miche parameter for saturated inner surf and swash derived by Baldock and Holmes [1999]. In contrast, for unsaturated surf conditions, the terminal bore height at the shoreline can be approximated by $H_b \approx 0.12 H_o$ which is consistent with recent independent laboratory data sets.

Acknowledgements

The assistance of Dave Mitchell, Felicia Weir, Andrew Aouad, Aart Kroon, Nick Cartwight, Dave Callaghan and PhD students at UQ on field trips is much appreciated. The authors are grateful to the Queensland Government, Manly Hydraulics Laboratory, and Danish Coastal Authority for supplying offshore wave data. Useful and constructive review comments from the associate editor Gerben Ruessink and Alex Apotsos helped improve the manuscript.

References

Aagaard, T., and G. Masselink (1999), The Surf Zone, in *Handbook of Beach and Shoreface Morphodynamics*, edited by A. D. Short, pp. 72-118, John Wiley and Sons, Chichester, United Kingdom.

Aagaard, T., A. Kroon, M. G. Hughes, and B. Greenwood (2008), Field observations of nearshore bar formation, *Earth Surface Processes and Landforms*, *33*(7), 1021-1032.

Alsina, J. M., and T. E. Baldock (2007), Improved representation of breaking wave energy dissipation in parametric wave transformation models, *Coastal Engineering*, *54*, 765-769.

Apotsos, A., B. Raubenheimer, S. Elgar, R. T. Guza, and J. A. Smith (2007), Effects of wave rollers and bottom stress on wave setup, *Journal of Geophysical Research*, *112*, C02003.

Baldock, T. E., P. Holmes, S. Bunker, and P. Van Weert (1998), Cross-shore hydrodynamics within an unsaturated surf zone, *Coastal Engineering*, *34*, 173-196.

Baldock, T. E., and P. Holmes (1999), Simulation and prediction of swash oscillations on a steep beach, *Coastal Engineering*, *36*(3), 219-242.

Baldock, T. E., and D. A. Huntley (2002), Long-wave forcing by the breaking of random gravity waves on a beach, *Proceedings of the Royal Society A: Mathematical, Physical and Engineering Sciences*, *458*(2025), 2177-2201.

Battjes, J. A. (1974), Surf similarity, paper presented at Proceedings of the 14th International Conference on Coastal Engineering, American Society of Civil Engineers, New York.

Battjes, J. A., and J. P. Janssen (1978), Energy loss and setup due to breaking of random waves, paper presented at Proceedings of the 16th International Conference on Coastal Engineering, American Society of Civil Engineers, New York.

Battjes, J. A., and M. J. F. Stive (1985), Verification of a dissipation model for random breaking waves., *Journal of Geophysical Research*, *90*(C5), 9159-9167.

Battjes, J. A. (1988), Surf-zone dynamics, *Annual Reveiw of Fluid Mechanics*, *20*, 257-293.

Battjes, J. A., and H. W. Groenendijk (2000), Wave height distributions on shallow foreshores, *Coastal Engineering*, *40*(3), 161-182.

Battjes, J. A., H. J. Bakkenes, T. T. Janssen, and A. R. van Dongeren (2004), Shoaling of subharmonic gravity waves, *Journal of Geophysical Research*, *109*, C02009.

Bradshaw, M. (1982), *Bores and swash on natural beaches*, Coastal Studies Unit Technical Report No. 82/4, Sydney.

Brocchini, M., and T. E. Baldock (2008), Recent advances in modeling swash zone dynamics: Influence of surf-swash interaction on nearshore hydrodynamics and morphodynamics, *Reviews of Geophysics*, *46*, RG3003.

Dean, R. G. (1991), Equilibrium Beach Profiles: Characteristics and Applications, *Journal of Coastal Research*, *7*(1), 53-84.

Dean, R. G., and R. A. Dalrymple (2002), *Coastal Processes with Engineering Applications*, 475 pp., Cambridge University Press, Cambridge.

Goda, Y. (1975), Irregular wave deformation in the surf zone, *Coastal Engineering in Japan*, *18*, 13-26.

Goda, Y. (1998), An overview of coastal engineering with emphasis on random wave approach, *Coastal Engineering Journal*, *40*(1), 1-21.

Goda, Y. (2004), A 2-D random wave transformation model with gradational breaker index, *Coastal Engineering Journal*, *46*(1), 1-38.

Horn, D. P., and T. Mason (1994), Swash zone sediment transport modes, *Marine Geology*, *120*(3-4), 309-325.

Hughes, M. G. (1992), Application of a Non-Linear Shallow Water Theory to Swash Following Bore Collapse on a Sandy Beach, *Journal of Coastal Research*, *8*(3), 562-578.

Hughes, M. G., and I. L. Turner (1999), The Beachface, in *Handbook of Beach and Shoreface Morphodynamics*, edited by A. D. Short, pp. 119-144, John Wiley and Sons, Chichester, United Kingdom.

Hughes, M. G., and A. S. Moseley (2007), Hydrokinematic regions within the swash zone, *Continental Shelf Research*, *27*(15), 2000-2013.

Janssen, T. T., and J. A. Battjes (2007), A note on wave energy dissipation over steep beaches, *Coastal Engineering*, *54*(9), 711-716.

Kobayashi, N., and B. D. Johnson (2001), Sand suspension, storage, advection, and settling in surf and swash zones, *Journal of Geophysical Research*, *106*(C5), 9363-9376.

Kobayashi, N., A. Payo, and L. Schmied (2008), Cross-shore suspended sand and bed load transport on beaches, *Journal of Geophysical Research*, *113*, C07001.

Komar, P. D. (1998), *Beach Processes and Sedimentation*, 2nd ed., 544 pp., Prentice Hall, New Jersey.

Masselink, G., and B. Hegge (1995), Morphodynamics of meso- and macrotidal beaches: examples from central Queensland, Australia, *Marine Geology*, *129*, 1-23.

Masselink, G., and J. A. Puleo (2006), Swash-zone morphodynamics, *Continental Shelf Research*, *26*(5), 661-680.

Nielsen, P. (1989), Wave setup and runup: An integrated approach, *Coastal Engineering*, *13*(1), 1-9.

Nielsen, P. (2009), *Coastal and estuarine processes*, 343 pp., World Scientific, Singapore.

Peregrine, D. H. (1974), Water-wave interaction in the surf zone, paper presented at Proceedings of the 14th International Conference on Coastal Engineering, American Society of Civil Engineers, New York.

Peregrine, D. H. (1983), Breaking Waves on Beaches, *Annual Review of Fluid Mechanics*, *15*(1), 149.

Puleo, J. A., K. T. Holland, N. G. Plant, D. N. Slinn, and D. M. Hanes (2003), Fluid acceleration effects on suspended sediment transport in the swash zone, *Journal of Geophysical Research*, *108*(C11), 3350.

Raubenheimer, B., R. T. Guza, and S. Elgar (1996), Wave transformation across the inner surf zone, *Journal of Geophysical Research*, *101*(C11), 25589-25597.

Raubenheimer, B., R. T. Guza, and S. Elgar (2001), Field observations of wave-driven setdown and setup, *Journal of Geophysical Research*, *106*(C3), 4629-4638.

Raubenheimer, B. (2002), Observations and predictions of fluid velocities in the surf and swash zone, *Journal of Geophysical Research*, *107*(C11), 3190-3196.

Ruessink, B. G., K. T. Houwman, and P. Hoekstra (1998), The systematic contribution of transporting mechanisms to the cross-shore sediment transport in water depths of 3 to 9 m, *Marine Geology*, *152*(4), 295-324.

Ruessink, B. G., D. J. R. Walstra, and H. N. Southgate (2003), Calibration and verification of a parametric wave model on barred beaches, *Coastal Engineering*, *48*(3), 139-149.

Ruggiero, P., R. A. Holman, and R. A. Beach (2004), Wave run-up on a high-energy dissipative beach, *Journal of Geophysical Research*, *109*(C06025).

Sallenger, A. H., and R. A. Holman (1985), Wave Energy Saturation on a Natural Beach of Variable Slope, *Journal of Geophysical Research*, *90*(C6), 11939-11944.

Sallenger, A. H., and P. A. Howd (1989), Nearshore bars and the break-point hypothesis, *Coastal Engineering*, *12*, 301-313.

Sénéchal, N., H. Dupuis, P. Bonneton, H. Howa, and R. Pedreros (2001), Observation of irregular wave transformation in the surf zone over a gently sloping sandy beach on the French Atlantic coastline, *Oceanologica Acta*, *24*(6), 545-556.

Sénéchal, N., V. Rey, P. Bonneton, and H. Dupuis (2005), On the difficulty of correctly determine the characteristic wave period in the surf zone, paper presented at Coastal Dynamics, American Society of Civil Engineers, New York.

Srinivas, R., and R. G. Dean (1996), Cross-shore hydrodynamics and profile response modeling, *Coastal Engineering*, *27*(3-4), 195-221.

Svendsen, I. A. (1984), Wave heights and set-up in a surf zone, *Coastal Engineering*, *8*, 303-329.

Thornton, E. B., and R. T. Guza (1982), Energy saturation and phase speeds measured on a natural beach, *Journal of Geophysical Research*, *87*(C12), 9499-9508.

Thornton, E. B., and R. T. Guza (1983), Transformation of Wave Height Distribution, *Journal of Geophysical Research*, *88*(C10), 5925-5938.

van der Westhuysen, A. J. (2010), Modelling of depth-induced wave breaking under finite-depth wave growth conditions, *Journal of Geophysical Research*, *115*(C1), C01008.

Weishar, L. L., and R. J. Byrne (1978), Field study of breaking wave characteristics, paper presented at Proceedings of the 16th International Conference on Coastal Engineering, American Society of Civil Engineers, New York.

Wright, L. D., P. Nielsen, A. D. Short, and M. O. Green (1982), Morphodynamics of a macrotidal beach, *Marine Geology*, *50*, 97-128.

Wright, L. D., and A. D. Short (1984), Morphodynamic variabililty of surf zones and beaches: a synthesis, *Marine Geology*, *56*, 93-118.

Tables

Table 1. Location, date, number of 15-minute data records (n), maximum number of PTs in the surf zone in one data record (n PTs), sampling frequency (f_s), beach slope in the inner surf zone ($\tan\beta$), mean offshore significant wave height (H_o), depth where offshore wave height was recorded (h_o), mean offshore wave period (T_z), offshore Iribarren number (ξ_o), maximum root-mean-square wave height in the inner surf zone (max H_{rms}), and mean period in the inner surf zone ($\overline{T}$), for each deployment. All beaches are in Australia unless otherwise indicated.

Location	Date	n	n PTs	f_s (Hz)	$\tan\beta$	H_o (m)	h_o (m)	T_z (s)	ξ_o	max H_{rms} (m)	$\overline{T}$ (s)
Seven Mile Beach (S.C.), N.S.W.	13 Nov. 2002	10	1	5	0.028	2.18	78	5.52	0.24	0.31	9.23
Seven Mile Beach (S.C.), N.S.W.	14 Nov. 2002	17	2	5	0.028	1.26	78	4.71	0.27	0.31	9.81
Seven Mile Beach (S.C.), N.S.W.	17 Nov. 2002	14	2	5	0.032	1.63	78	6.11	0.52	0.37	13.39
Seven Mile Beach (S.C.), N.S.W.	18 Nov. 2002	18	2	5	0.028	0.93	78	3.80	0.25	0.27	10.00
Seven Mile Beach (S.C.), N.S.W.	19 Nov. 2002	20	2	5	0.028	0.96	78	4.43	0.32	0.28	8.43
Seven Mile Beach (S.C.), N.S.W.	21 Nov. 2002	18	2	5	0.028	1.76	78	5.07	0.22	0.31	6.04
One Mile Beach, N.S.W.	6 May 2004	5	5	5	0.044	2.56	79	7.55	0.22	0.46	12.74
Bluey’s Beach, N.S.W.	7 May 2004	5	5	5	0.033	1.64	79	8.26	0.11	0.49	14.10
Elizabeth Beach , N.S.W.	11 May 2004	14	4	5	0.034	1.98	79	6.27	0.19	0.38	11.89
Avoca Beach, N.S.W.	16 Nov. 2004	18	9	10	0.072	1.65	85	6.15	0.43	0.61	5.65
Avoca Beach, N.S.W.	17 Nov. 2004	19	9	10	0.082	1.14	85	6.34	0.61	0.61	6.59
Vejers Beach, Denmark	4 Oct. 2006	48	2	8	0.017	1.34	16	4.28	0.08	0.49	3.98
Vejers Beach, Denmark	5 Oct. 2006	37	1	8	0.020	1.35	16	4.31	0.09	0.45	3.71
Vejers Beach, Denmark	7 Oct. 2006	52	2	8	0.019	2.71	16	5.48	0.08	0.80	4.29
Boomerang Beach, N.S.W.	24 Apr. 2007	10	4	5	0.023	1.41	79	5.73	0.09	0.46	11.44
Seven Mile Beach (C.C.), N.S.W.	26 Apr. 2007	12	4	5	0.031	1.65	79	6.35	0.17	0.67	8.53
Bluey's Beach, N.S.W.	27 Apr. 2007	15	1	5	0.038	1.34	79	6.88	0.19	0.67	6.97
Moreton Island, Qld.	10 Dec. 2007	35	14	4	0.046	0.89	76	5.89	0.23	0.43	7.44
Moreton Island, Qld.	11 Dec. 2007	32	11	4	0.029	0.80	76	5.40	0.22	0.35	6.24
The Spit, Qld.	1 Oct. 2008	12	8	10	0.029	0.99	18	4.69	0.20	0.33	7.06
The Spit, Qld.	18 Nov. 2008	19	7	10	0.048	1.16	18	5.11	0.38	0.32	6.32
Moreton Island, Qld.	7 Dec. 2008	11	11	10	0.027	0.75	76	3.83	0.15	0.24	6.09
Moreton Island, Qld.	8 Dec. 2008	19	11	10	0.033	1.00	76	4.52	0.19	0.36	6.37
Moreton Island, Qld.	9 Dec. 2008	17	10	10	0.032	1.24	76	5.63	0.21	0.37	7.34
The Spit, Qld.	10 Mar. 2009	18	4	10	0.033	2.97	18	6.29	0.12	0.37	11.33
The Spit, Qld.	11 Mar.2009	17	6	10	0.054	3.01	18	6.95	0.21	0.53	10.84
The Spit, Qld.	12 Mar.2009	13	3	10	0.046	2.33	18	6.15	0.22	0.47	10.80

Figure Captions

Figure 1. Representative cross-shore profiles for each beach: (a) Seven Mile Beach (South Coast), (b) One Mile Beach, (c) Bluey's Beach, (d) Elizabeth Beach, (e) Avoca Beach, (f) Vejers Beach, (g) Boomerang Beach, (h) Seven Mile Beach (Central Coast), (i) Moreton Island, and (j) The Spit. Profiles for multiple deployments at the same beach are not shown, but do not vary significantly All profiles are shown with 12x vertical exaggeration.

Figure 2. Histogram of $\bar{h}/H_o$ for each data record from all deployments.

Figure 3. Comparison of (a) original water surface elevation (▬) and its mean (· · ·), with (b) high-pass fast Fourier filtered data record (▬). The zero line is shown (· · ·). The location of the troughs (○) and peaks (□) on each data record are shown. The troughs and peaks on the original water surface elevation were calculated using the local minima analysis and the troughs and peaks on the fast Fourier transform filtered data record were calculated using a zero down-crossing analysis.

Figure 4. (a) Comparison of γ_{rms} and offshore wave height for all data and (b) comparison of γ_{rms} and offshore wave height for all data with data binned according to water depth for $0.5 < h < 1.0$m (Δ), $1.0 < h < 1.5$m (○), $1.5 < h < 2.0$m (□), and $h > 2.0$m (◊).

Figure 5. Comparison of γ_{rms} and mean water depth ($\bar{h}$) for six deployments: (a) Seven Mile Beach (18/11/02), (b) Avoca Beach (16/11/04), (c) Vejers Beach (05/10/06), (d) Moreton Island (10/12/07), (e) Moreton Island (08/12/08), and (f) The Spit (12/03/09).

Figure 6. Comparison of γ_s and (a) normalized beach slope $\beta/k_{pf}\bar{h}$, (b) local β, (c) h, (d) $1/h$, (e) k_{pf} and (f) $1/T_{pf}$ following the method of Raubenheimer *et al*. [1996]. Data are binned corresponding to $\beta/k\bar{h} \pm 0.025$, $\beta \pm 0.0025$, $h \pm 0.05$, $1/h \pm 0.125$, $k_{pf} \pm 0.025$ and $1/T_{pf} \pm 0.005$. The mean and standard deviation of each bin range is shown (●) and values for individual data records (●; plots b-f). The least squares linear fit ($\gamma_s = (0.19 \pm 0.09) + (1.05 \pm 0.15)\beta/k_{pf}\bar{h}$) from Raubenheimer *et al*. [1996] is also shown in (a) (- - -).

Figure 7. Comparison of γ_s and (a) normalized beach slope $\beta/\bar{k}\bar{h}$, (b) $\bar{k}$ and (c) $1/T$ using the method of Raubenheimer *et al*. [1996] to calculate γ_s and the local minima analysis to obtain values for $\bar{T}$. Data are binned corresponding to $\beta/\bar{k}\bar{h} \pm 0.025$, $\bar{k} \pm 0.025$ and $1/\bar{T} \pm 0.005$. The mean and standard deviation of each bin range is shown (●) and values for individual data

records (●; plots b-c). The least squares linear fit ($\gamma_s = (0.19 \pm 0.09) + (1.05 \pm 0.15)\beta / k_{pf}\bar{h}$) from Raubenheimer *et al*. [1996] is also shown in (a) (- - -).

Figure 8. Comparison of the three different methods that have been used to calculate gamma: (a)-(b) γ_{rms}, (c)-(d) $\bar{\gamma}_w$, and (e)-(f) $\bar{\gamma}_{tr}$ plotted against mean water depth ($\bar{h}$) normalized by the offshore wave height (H_o). Each point represents a 15 minute data record. The plots shown on the left are from Avoca Beach (16/11/04) and the plots shown on the right are from Moreton Island (10/12/07).

Figure 9. Comparison of (a) $\bar{\gamma}_{tr}$ and mean water depth ($\bar{h}_{tr}$) and (b) $\bar{\gamma}_w$ and mean depth of the wave ($\bar{h}_w$), normalized by the offshore wave height (H_o) for all data.

Figure 10. Comparison of at $\bar{\gamma}_w$-values and $\bar{h}_{tr}$ for all data (●). The empirical equation $\gamma_w = \dfrac{2}{\left(1 + 20\bar{h}_{tr}/H_o\right)^{0.75}}$ ($R^2 = 0.77$) is shown (▬) such that $\bar{\gamma}_w = 2$ at $\bar{h}_{tr}/H_o = 0$.

Figure 11. Example histograms of the skewness of (a) γ_w- values and (b) γ_{tr}-values for all the waves at one location over a 15-minute data record at Avoca Beach (16/11/04), Record 28, PT 7.

Figure 12. Histogram of the skewness of γ_{tr}-values for each data record from all instrument deployments.

Figure 13. Histogram of all the (a) γ_w-values and (b) γ_{tr}-values for individual waves from all data.

Figure 14. Wave height for individual waves plotted against mean water depth of the wave (h_w) and trough depth (h_{tr}) for (a)-(b) Avoca Beach 16/11/04, (c)-(d) Vejers Beach 07/10/06, and (e)-(f) Moreton Island (10/12/07). Each color in each plot represents data from a different location. The lines of $\gamma = 0{:}5$ (- - -), $\gamma = 1$ (▬), and $\gamma = 1{:}5$ (· · ·) are shown.

Figure 15. Comparison of $\bar{\gamma}_w$ and $H_o/\bar{h}_w$ for all data sets (●). The line of best fit ($\gamma_w = 0.11 H_o/h_w + 0.11$; $R^2 = 0.73$, · · ·) and the best fit power curve ($\gamma_w = 0.22\left(H_o/h_w\right)^{0.63}$; $R^2 = 0.74$, ▬) are shown.

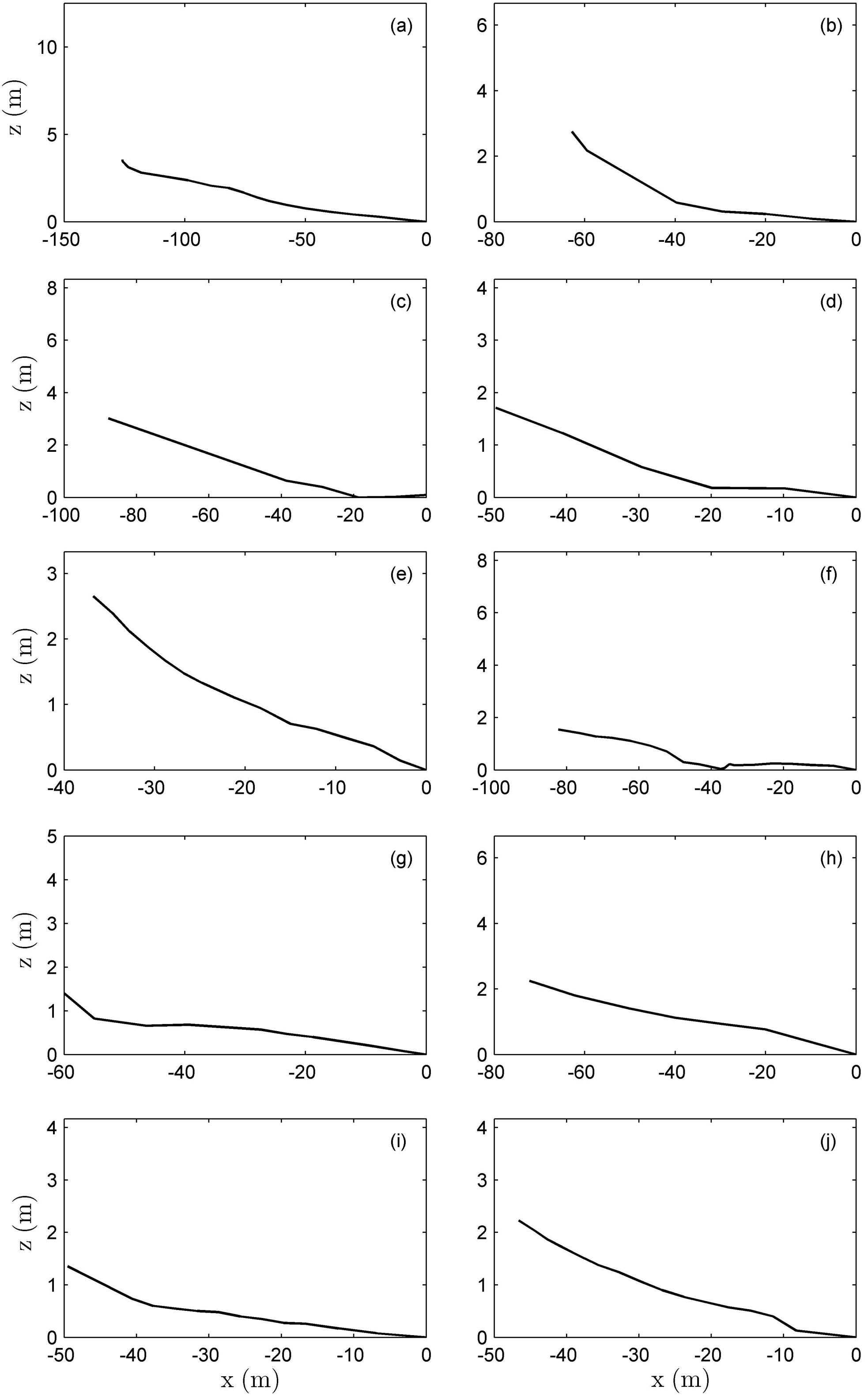

(a)
(b)
(c)
(d)
(e)
(f)
(g)
(h)
(i)
(j)
z (m)
x (m)

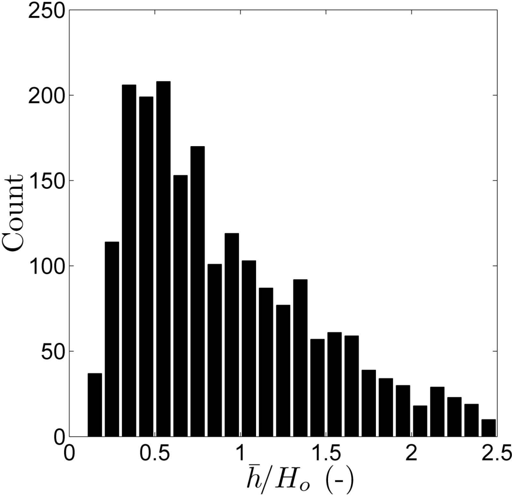

250
200
150
100
50
0
Count
0
0.5
1
1.5
2
2.5
$\bar{h}/H_o$ (-)

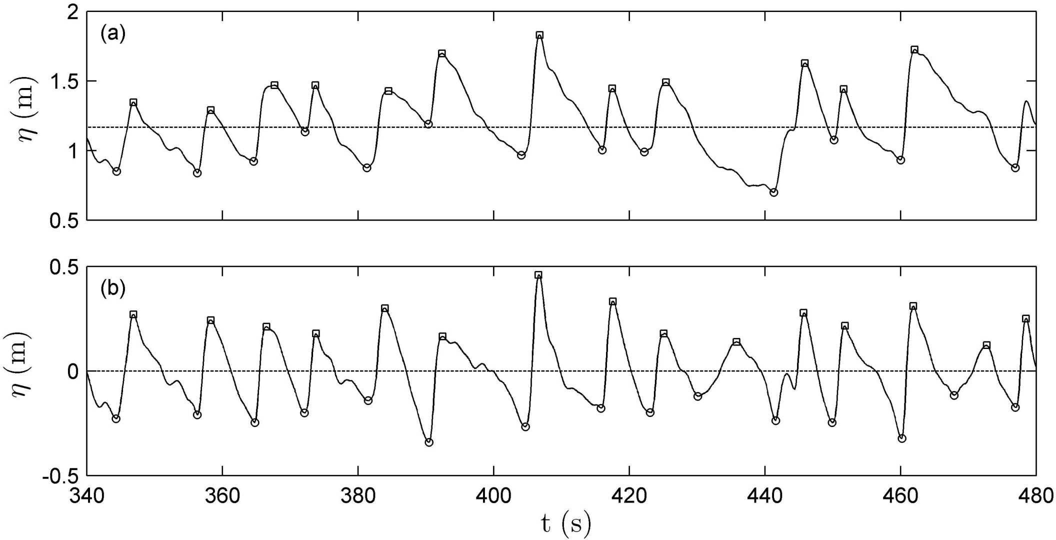

(a)
(b)
η (m)
η (m)
t (s)
2
1.5
1
0.5
0.5
0
-0.5
340
360
380
400
420
440
460
480

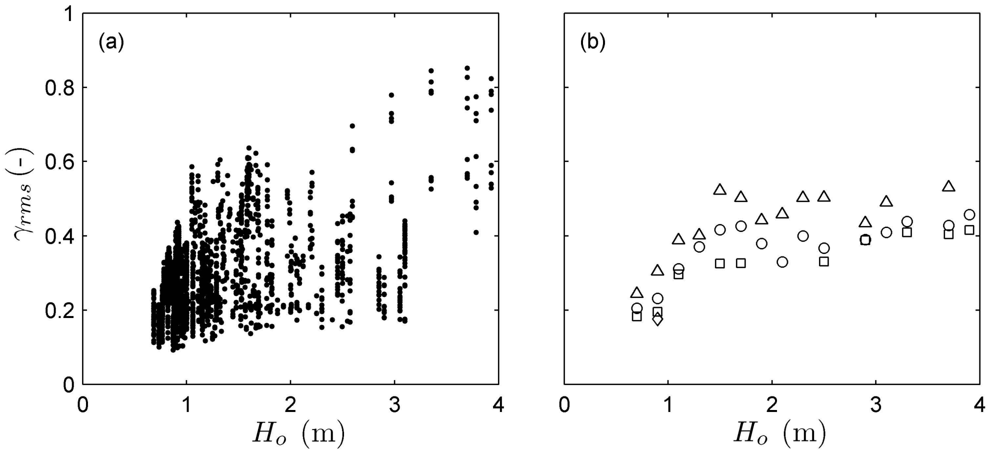

(a)
(b)
γ_{rms} (-)
H_o (m)
H_o (m)
0
0.2
0.4
0.6
0.8
1
0
1
2
3
4

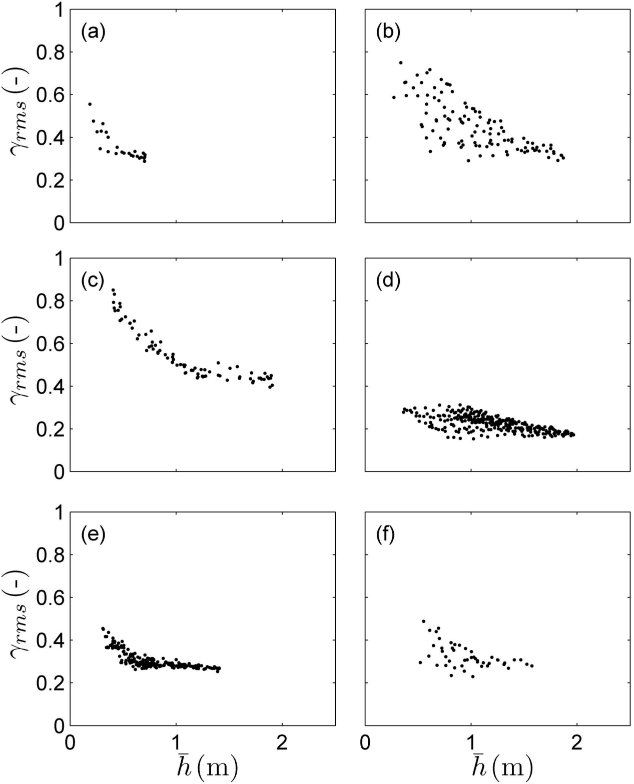
(a)
(b)
(c)
(d)
(e)
(f)
γ_{rms} (-)
$\bar{h}$ (m)
0
0.2
0.4
0.6
0.8
1
0
1
2

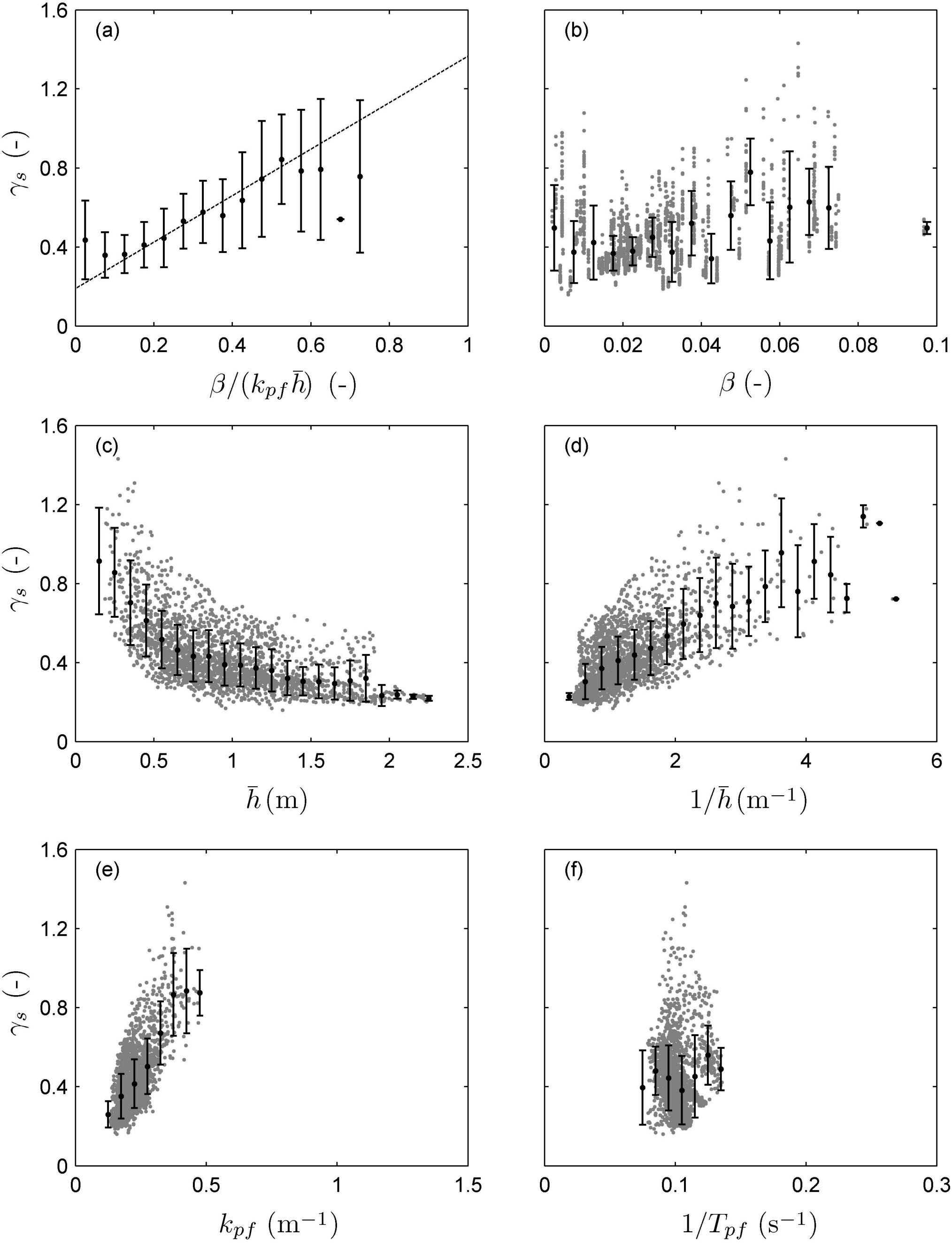

(a)
(b)
(c)
(d)
(e)
(f)
γ_s (-)
$\beta/(k_{pf}\bar{h})$ (-)
β (-)
$\bar{h}\,(\mathrm{m})$
$1/\bar{h}\,(\mathrm{m}^{-1})$
k_{pf} (m^{-1})
$1/T_{pf}$ (s^{-1})

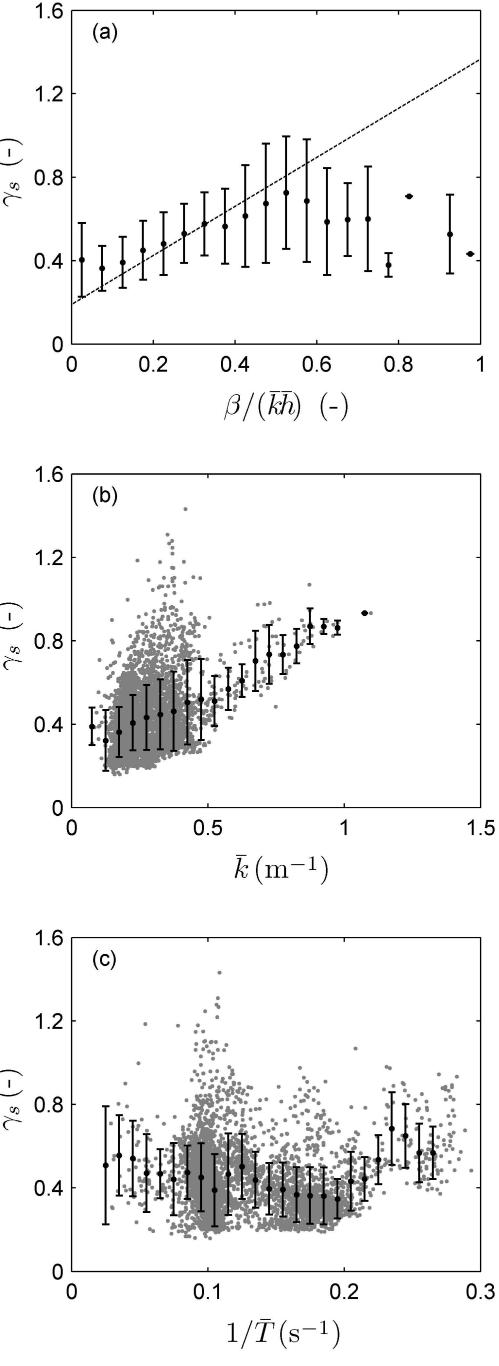

(a)
(b)
(c)
1.6
1.2
0.8
0.4
0
γ_s (-)
0 0.2 0.4 0.6 0.8 1
$\beta/(\bar{k}\bar{h})$ (-)
0 0.5 1 1.5
$\bar{k}\,(\mathrm{m}^{-1})$
0 0.1 0.2 0.3
$1/\bar{T}\,(\mathrm{s}^{-1})$

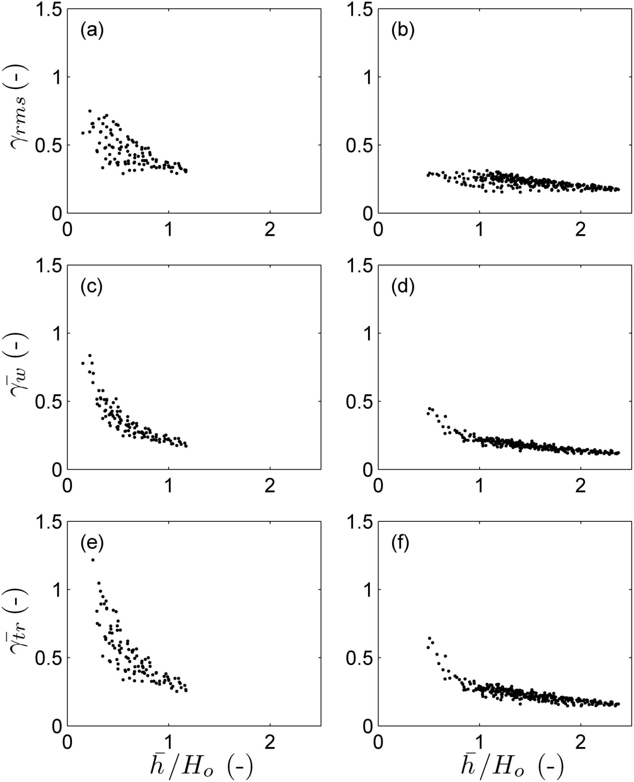

(a)
(b)
(c)
(d)
(e)
(f)
γ_{rms} (-)
$\gamma_{\bar{w}}$ (-)
$\gamma_{\bar{tr}}$ (-)
$\bar{h}/H_o$ (-)
$\bar{h}/H_o$ (-)
0
0.5
1
1.5
0
1
2

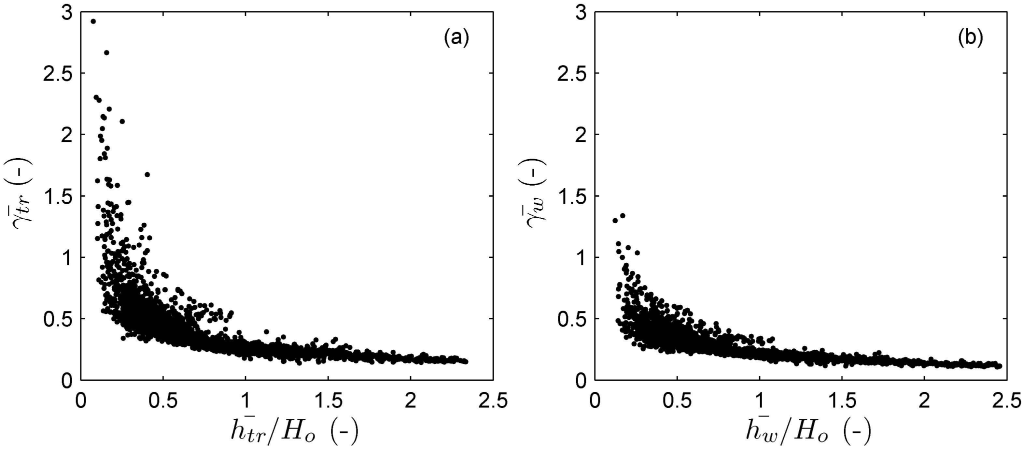

(a)
(b)
$\bar{\gamma_{tr}}$ (-)
$\bar{h_{tr}}/H_o$ (-)
$\bar{\gamma_w}$ (-)
$\bar{h_w}/H_o$ (-)
0
0.5
1
1.5
2
2.5
3

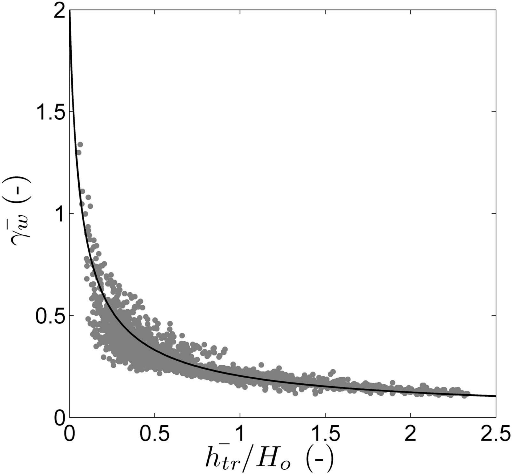

2
1.5
1
0.5
0
$\gamma_{\bar{w}}$ (-)
0
0.5
1
1.5
2
2.5
$h_{\bar{tr}}/H_o$ (-)

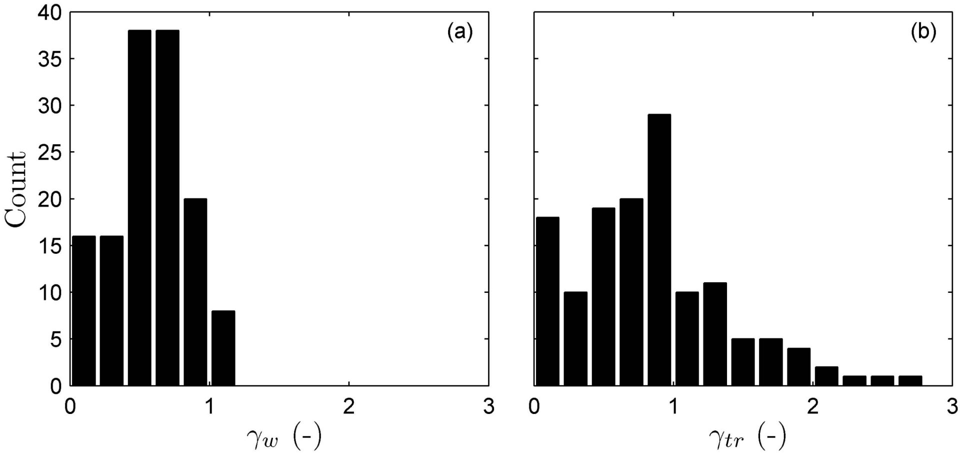

(a)
(b)
Count
0
5
10
15
20
25
30
35
40
0
1
2
3
γ_w (-)
γ_{tr} (-)

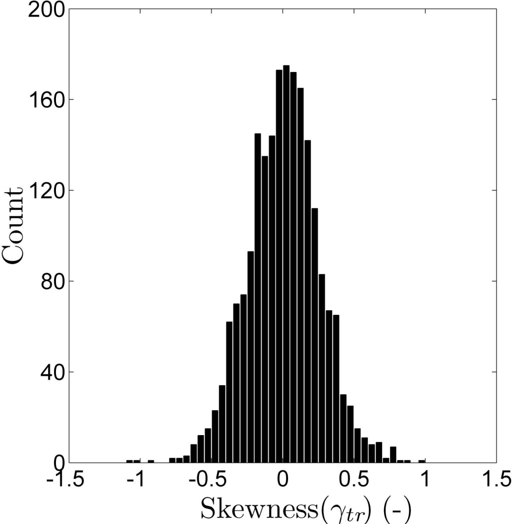

200
160
120
80
40
0
Count
-1.5
-1
-0.5
0
0.5
1
1.5
Skewness(γ_{tr}) (-)

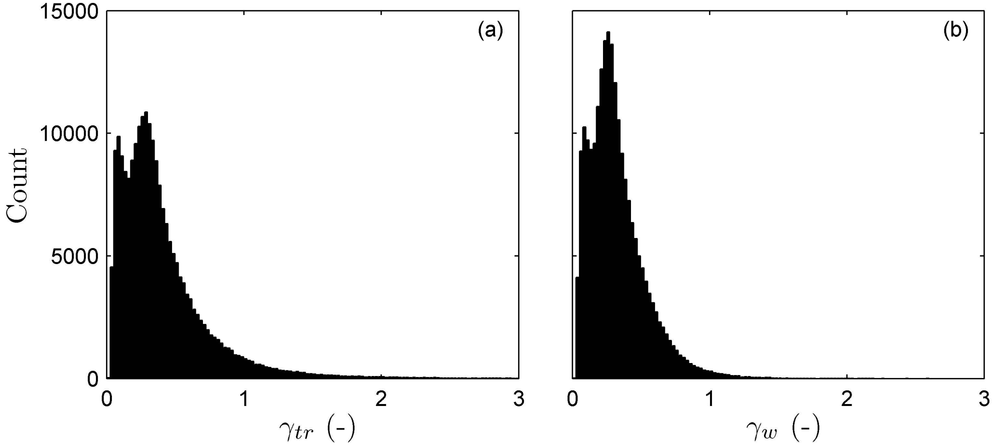
(a)
(b)
Count
15000
10000
5000
0
0
1
2
3
γ_{tr} (-)
γ_w (-)

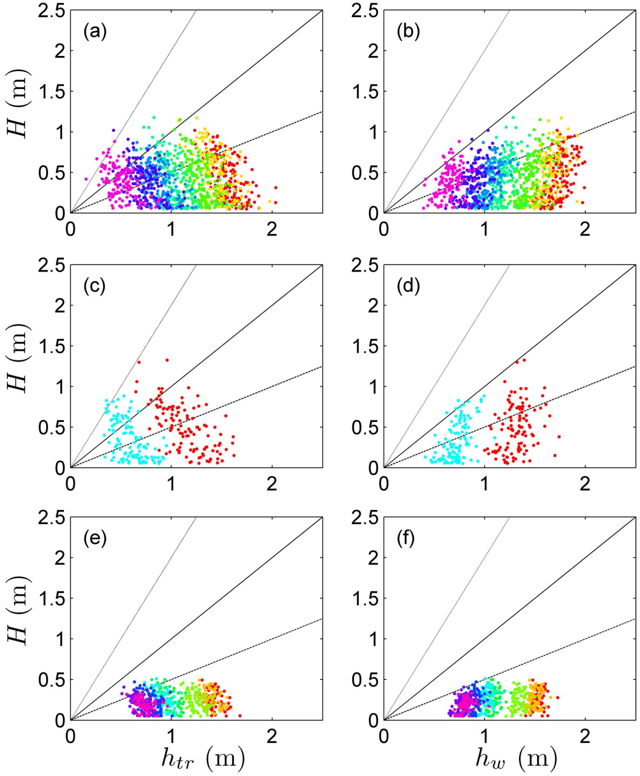

(a)
(b)
(c)
(d)
(e)
(f)
H (m)
h_tr (m)
h_w (m)
0
0.5
1
1.5
2
2.5

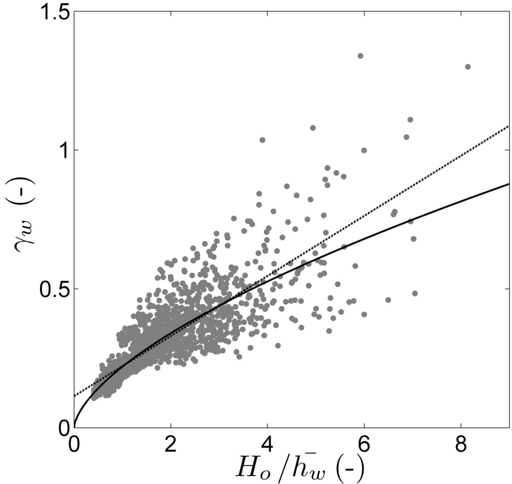

1.5
1
0.5
0
γ_w (-)
0
2
4
6
8
H_o/h_w^- (-)